A Multi-Agent System Based Hierarchical Control Framework for Microgrids

Mengxiang Liu[1], Zheyuan Cheng[2], Zhenyong Zhang[1], Mingyang Sun[1], Ruilong Deng[1], Peng Cheng[1] and Mo-Yuen Chow[2]

***Abstract*— The Microgrid is one of the most cost-effective solutions for integrating Distributed Energy Resources (DERs) into distribution systems. The hierarchical control framework, which typically includes primary, secondary and tertiary control layers, is adopted in the Microgrid to meet the control requirements of different spatial and time scales. Given the growing concern on the centralized control framework's scalability and robustness, the distributed control framework has become an indispensable development trend. In this paper, we propose a Multi-Agent System (MAS) based hierarchical control framework for Microgrids, where each agent consists of a series of DERs (i.e., distributed generations, storage units and loads). In the proposed framework, each agent has its specific task for regulating the local output voltage, and will collaborate with neighbors to achieve the overall objective of Microgrids in a totally distributed manner. Through extensive simulations and experiments, it is demonstrated that the proposed framework possesses high robustness to link failures and good scalability.**

I. INTRODUCTION

It is well recognized that installing distributed energy resources (DERs) at the distribution system level will become a general trend due to its technical and economical feasibility and sustainable development potential [1]. High penetrations of DERs such as solar photovoltaics (PVs), fuel cells and microturbines have transformed the regulated power generations into restructured entities [2]. The Microgrid has appeared as one of the most promising solutions to integrate DERs into distribution systems, with which the power system could operate in a more stable, efficient and economic manner. The concept of Microgrid is formally defined as the composition of distributed generations together with storage devices (flywheels, energy capacitors or batteries) and flexible loads in the distribution system [3]. The Microgrid will operate in a non-autonomous way, if interconnected to the grid, or in an autonomous way, if disconnected from the main grid. It is expected that components in the Microgrid should work in a collaborative manner to provide distinct benefits to the overall system performance, like improving the power quality or reducing the transmission losses [4].

This work was supported partially by the National Natural Science Foundation of China under Grants 62073285, 61833015, and 61903328, and partially by the National Science Foundation under CNS-1505633.

[1]Mengxiang Liu, Zhenyong Zhang, Mingyang Sun, Ruilong Deng, and Peng Cheng are with State Key Lab. of Industrial Control Technology, Zhejiang University, Hangzhou, 310027, P. R. China. Emails: {lmx329, zhangzhenyong, mingyangsun, dengruilong, lunarheart}@zju.edu.cn

[2]Zheyuan Cheng and Mo-Yuen Chow are with the Department of Electrical and Computer Engineering, North Carolina State University, Raleigh. Emails: {zcheng3, chow}@ncsu.edu

To meet the control requirements of different spatial and time scales (such as the interoperability of DERs), the hierarchical control framework, which typically includes the primary, secondary and tertiary control layers, is adopted in the Microgrid [5]. Specifically, the primary control layer maintains the voltage and frequency stability of the Microgrid subsequent to the islanding process; the secondary control layer compensates for the voltage and frequency deviations induced in the primary control layer; and the tertiary control layer manages the power flow between the Microgrid and the main grid in order to facilitate an economically optimal operation [6].

Traditional distribution systems employ the centralized supervisory control and data acquisition (SCADA) system to monitor, protect and control equipments with the help of advanced information communication technologies. Nevertheless, the centralized SCADA system may be inadequate in integrating large amount of DERs into the future distribution system due to its shortcomings in scalability and flexibility [7]. Given that each DER is typically equipped with the intelligent power electronic device (converter/inverter) and communication interfaces, it is favorable to leverage these DERs' local resources to perform computing tasks such that the need for a control center can be eliminated [8]. The methodology of Multi-Agent System (MAS) has been widely recognized as a feasible and efficient approach for managing complex DERs in a distributed fashion. Compared with the traditional centralized approaches, the MAS approach has countless advantages like the increased scalability and robustness, the reduced need for large data manipulation, and etc [9].

Numerous research works have been devoted to applying the MAS approach into the Microgrid ranging from the secondary control layer to the tertiary control layer. In the secondary control layer, based on the distributed cooperative control of MASs, Bidram *et al.* propose a secondary voltage and frequency control scheme for Microgrids [10]; Further, consider the nature of uncertainty and intermittency in the DERs, Zhou *et al.* propose an agent-based secondary H_∞ consensus approach with an event-triggered communication scheme for Micorgrids [11]. As for the tertiary control layer, Hu *et al.* apply the multi-agent technology into the electric power distribution system congestion management considering the integration of electric vehicles [12]; From the perspective of cyber security, Duan *et al.* propose a resilient agent-based DC optimal Power Flow (OPF) algorithm against data integrity attacks [13], and Cheng *et al.* propose a

resilient collaborative agent-based AC OPF algorithm against false data injection attacks [14]. Moreover, Duan *et al.* consider the impact of packet losses and propose a robust agent-based distributed energy management algorithm for Microgrids [15].

However, existing literatures focus on either the secondary control layer or the tertiary control layer when utilizing the MAS technology, while the framework accommodating the three control layers has not been well investigated yet. Towards this end, we propose an MAS-based hierarchical control framework for Microgrids, where each agent has its specific task and collaborates with neighbors to achieve the overall objective in a totally distributed manner. Moreover, extensive simulations and experiments are conducted to demonstrate that the proposed framework possesses the following two advantages compared with the traditional centralized control framework: 1) High robustness to link failures: The Microgrid can still achieve voltage balancing and current sharing even under link failures as long as the communication network is connected; 2) Good scalability: The total computation time before convergence grows linearly as the number of agents grows. Hence, it is positive to expect the proposed framework could be promisingly adopted in the future distribution system with the high penetration of distributed energy resources and the rapid development of information communication technologies.

The remainder of this paper is organized as follows. In Section II, we introduce the concept of MAS. In Section III, we present the MAS-based hierarchical control framework for Microgrids. We show the simulation and experiment results in Section IV, and Section V concludes this paper.

II. The Concept of MAS

In this section, we introduce the concept of MAS, which is formally defined by the IEEE Power Engineering MAS working group [16]. The basic component of MAS, i.e., the agent, is merely a software (or hardware) entity that is suited in some environment and is able to autonomously react to changes in that environments. Here, the environment is everything outside the agent, and the property of autonomy means that the agent is able to schedule its actions based on observations from environment. In addition to the property of autonomy, the agent possessing the property of flexible autonomy is called the *intelligent agent*. In particular, the intelligent agent has the following three characteristics:

- ***Reactivity:*** an intelligent agent is able to react to changes in its environment in a timely fashion, and takes actions based on those changes and the designed functions.
- ***Pro-activeness:*** intelligent agents exhibit goal-directed behavior. Goal-directed behavior connotes that an agent will dynamically change its behavior in order to achieve its goals.
- ***Social ability:*** intelligent agents are able to interact with other intelligent agents. Social ability connotes more than the simple passing of data between different software and hardware entities, something many traditional systems do.

The MAS is simply a networked system comprising two or more agents or intelligent agents. Let graph $\mathcal{G} = \{\mathcal{A}, \mathcal{E}\}$ denote the coupling network among agents, where $\mathcal{A} = \{1, \cdots, N\}$ is the set of agents and $\mathcal{E} = \{1, \cdots, L\}$ is the set of coupling links/lines. Each $l = \{i, j\} \in \mathcal{E}$ connects agents i and j. Moreover, the set of agents coupled with agent i is denoted by $\mathcal{N}_i$.

III. MAS-based Hierarchical Control Framework for Microgrids

In this section, we model the Microgrid with the technology of MAS, and introduce the hierarchical control framework inside each agent. The agent is composed of a series of DERs including distributed generations, storage units and loads as shown in Fig. 1. The coupling networks among agents include the communication network $\mathcal{G}_c = \{\mathcal{A}, \mathcal{E}_c\}$ and the electrical network $\mathcal{G}_{el} = \{\mathcal{A}, \mathcal{E}_{el}\}$, where $\mathcal{E}_c$ and $\mathcal{E}_{el}$ denote the sets of communication links and electrical lines, respectively.

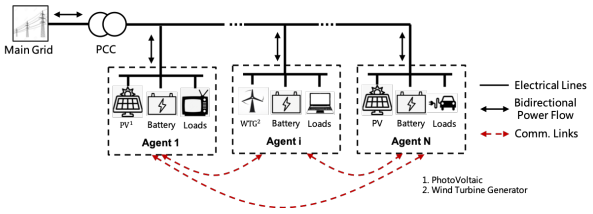

Fig. 1. This diagram depicts the MAS-based Microgrid, where each agent constitutes of a series of DERs including distributed generations, storage units and loads.

As shown in Fig. 2, each agent shares the secondary and tertiary control related information $\boldsymbol{x}_i^s, \boldsymbol{x}_i^t, \forall i \in \mathcal{N}_i^c$ with neighbors through communication links, and employs a local hierarchical control framework to complete its specific task, under which the overall objective of the Microgrid can be achieved. In particular, each layer has the duty of a command level and provides supervisory control over lower-layer systems [6]. In this regard, the command and reference signals from one layer to the lower layers should induce low impact in the stability and robustness performance, and thus the bandwidth will be decreased with an increase in the control layer. To simplify the design of control algorithms/parameters in each layer, it is feasible to consider that the command and reference signals from upper layers are constant and hence the system dynamics of each layer can be decoupled from other layers. In the context of Microgrids, each agent can react autonomously to environment changes (e.g., load variations and plugging-in/out of DERs) to maintain the voltage and frequency, and each agent has its specific task and collaborates with neighbors to achieve the overall objective, indicating that the intelligence (i.e., *reactivity*, *pro-activeness* and *social ability*) of agents is well reflected. Next, we will elaborate the detail of each control layer.

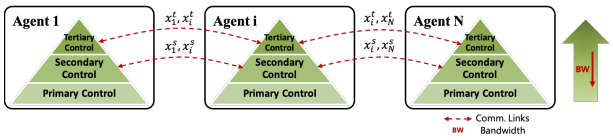

Fig. 2. This diagram depicts the MAS-based hierarchical control framework for Microgrids.

A. MAS-based Primary Control Layer

The primary control layer is to stabilize the voltage and frequency, to offer plug-and-play capability for DERs and properly share the loads among them, preferably, without communication links [17]. In terms of the control functionality, the primary control layer adjusts the amplitude and frequency of voltage reference applied to the inner current and voltage control loops. The main idea behind this control layer is to mimic the dynamics of a synchronous generator, which pulls down the frequency when the active power increases [18]. In AC Microgrids, the operation principle can be illustrated through the typical P/Q droop method:

$$\omega = \omega^* - D_P(P - P^*) \tag{1}$$
$$E = E^* - D_Q(Q - Q^*), \tag{2}$$

where ω, E denote the frequency and amplitude of the output voltage reference and ω^*, E^* are their references, D_P, D_Q are droop constants, P, Q are the output active and reactive power, and P^*, Q^* are their references. In DC Microgrids, the voltage versus current droop is

$$V = V^* - D_V(I - I^*), \tag{3}$$

where V denotes the output voltage reference and V^* is its reference, D_V is the droop constant, and I is the output current reference and I^* is its reference. It follows from (1)-(3) that each agent is able to implement the primary control layer utilizing merely the local measurements. Hence, within the primary control layer, the dynamics of agent $i \in \mathcal{A}$ are

$$\boldsymbol{u}_i^p(k+1) = \boldsymbol{f}_i^p(\boldsymbol{x}_i^p(k), \boldsymbol{u}_i^s, \boldsymbol{u}_i^t), \tag{4}$$

where $\boldsymbol{u}_i^p(k)$ denotes the reference voltage applied to inner loops inside the inverter, $\boldsymbol{u}_i^s$ and $\boldsymbol{u}_i^t$ signify the constant commands and reference signals from secondary and tertiary control layers. In most cases, $\boldsymbol{u}_i^s$ and $\boldsymbol{u}_i^t$ will regulate the references values like ω^*, E^*, and V^* to provide supervisory control over the primary control layer.

B. MAS-based Secondary Control Layer

With the help of the communication network, the secondary control layer is able to compensate the voltage and frequency deviations induced in the primary control layer. According to [10], [19], each agent employs a consensus-like algorithm for the production of compensation signals:

$$\boldsymbol{u}_i^s(k+1) = \sum_{j \in \mathcal{N}_i^c} w_{ij}(\boldsymbol{x}_i^s(k) - \boldsymbol{x}_j^s(k)) + g_i(\boldsymbol{x}_i^s(k) - \boldsymbol{u}_i^t), \tag{5}$$

where $\boldsymbol{x}_i^s(k)$ denote agent i's secondary control related variables (e.g., voltage, frequency, and active/reactive power.), w_{ij} is the weight of $(i,j) \in \mathcal{E}_c$ and g_i is the weight of the local regulation error. In mathematics, equation (5) aims to synchronize $\boldsymbol{x}_i^s, \forall i \in \mathcal{A}$ to the state determined by $\boldsymbol{u}_i^t, \forall i \in \mathcal{A}$, which in the Microgrid can be interpreted as to regulate the output voltage to the reference optimized by the tertiary control layer or to evenly share the active/reactive power among agents.

C. MAS-based Tertiary Control Layer

In the tertiary control layer, all agents work collaboratively to solve the AC OPF problem in a distributed manner. The AC OPF problem can be mathematically formulated as

$$\min_{\boldsymbol{x}^t} \; J(\boldsymbol{x}^t) \tag{6}$$
$$\text{s.t.} \boldsymbol{h}(\boldsymbol{x}^t) = \boldsymbol{0}, \boldsymbol{g}(\boldsymbol{x}^t) \leq \boldsymbol{0},$$

where the objective function is to minimize the total generation costs, $\boldsymbol{h}(\boldsymbol{x}^t) = \boldsymbol{0}$ denotes the equality constraints covering the power flow at each power line and power injection at each agent, and $\boldsymbol{g}(\boldsymbol{x}^t) \leq \boldsymbol{0}$ signifies the inequality constraints composed by generators' operational limits and branches' operational limits. The tertiary control related variable $\boldsymbol{x}^t$ includes agents' output active/reactive power references, output voltage references, and etc. After applying certain convex relaxations to constraints $\boldsymbol{h}(\boldsymbol{x})$ and $\boldsymbol{g}(\boldsymbol{x})$, the feasible set of (6) can be affine [20]. Hence, with the quadratic function $J(\boldsymbol{x})$, the OPF problem can be solved by utilizing the dual decomposition concept together with the primal-dual subgradient (PDS) approach. Specifically, we can construct the following Lagrangian function through multipliers and penalty terms:

$$\mathcal{L}(\boldsymbol{x}^t) = J(\boldsymbol{x}^t) + \boldsymbol{\lambda}\boldsymbol{h}(\boldsymbol{x}^t) + \boldsymbol{\mu}\boldsymbol{g}(\boldsymbol{x}^t)_+ + \\ + \frac{\rho}{2}||\boldsymbol{h}(\boldsymbol{x}^t)||_2^2 + \frac{\rho}{2}||\boldsymbol{g}(\boldsymbol{x}^t)||_2^2,$$

where $\boldsymbol{\lambda}, \boldsymbol{\mu}$ denote the Lagrangian multiplies (dual variables), ρ signifies the penalty factor, and function $(\cdot)_+$ is the positive projection. The optimal solution to problem (6) exists at the saddle point of the Lagrangian function $\mathcal{L}$. According to the PDS method in [21], we consider that the saddle point of the Lagrangian function can be reached by separately and iteratively moving the primal variables $\boldsymbol{x}^t$ towards negative gradient direction, whereas moving the dual variables $\boldsymbol{\lambda}, \boldsymbol{\mu}$ towards positive gradient direction, as defined by the following equations:

$$\boldsymbol{x}^t(k+1) = \boldsymbol{x}^t(k) - \xi \frac{\partial \mathcal{L}}{\partial \boldsymbol{x}^t}|_{\{\boldsymbol{x}^t(k), \boldsymbol{\lambda}(k), \boldsymbol{\mu}(k)\}}, \tag{7a}$$
$$\boldsymbol{\lambda}(k+1) = \boldsymbol{\lambda}(k) + \xi \frac{\partial \mathcal{L}}{\partial \boldsymbol{\lambda}}|_{\{\boldsymbol{x}^t(k), \boldsymbol{\lambda}(k), \boldsymbol{\mu}(k)\}}, \tag{7b}$$
$$\boldsymbol{\mu}(k+1) = \boldsymbol{\mu}(k) + \xi \frac{\partial \mathcal{L}}{\partial \boldsymbol{\mu}}|_{\{\boldsymbol{x}^t(k), \boldsymbol{\lambda}(k), \boldsymbol{\mu}(k)\}}, \tag{7c}$$

where ξ denotes the step size. With equations (7), the distributed OPF solver for agent $i \in \mathcal{A}$ can be obtained as

$$\boldsymbol{x}_i^t(k+1) = \boldsymbol{f}_i^x(\boldsymbol{x}_i^t(k), \boldsymbol{\lambda}_i(k), \boldsymbol{\mu}_i(k), \boldsymbol{x}_{\mathcal{N}_i}^t(k), \boldsymbol{\lambda}_{\mathcal{N}_i}(k), \boldsymbol{\mu}_{\mathcal{N}_i}(k)),$$
$$\boldsymbol{\lambda}_i(k+1) = \boldsymbol{f}_i^\lambda(\boldsymbol{x}_i^t(k), \boldsymbol{\lambda}_i(k), \boldsymbol{\mu}_i(k), \boldsymbol{x}_{\mathcal{N}_i}^t(k), \boldsymbol{\lambda}_{\mathcal{N}_i}(k), \boldsymbol{\mu}_{\mathcal{N}_i}(k)),$$
$$\boldsymbol{\mu}_i(k+1) = \boldsymbol{f}_i^\mu(\boldsymbol{x}_i^t(k), \boldsymbol{\lambda}_i(k), \boldsymbol{\mu}_i(k), \boldsymbol{x}_{\mathcal{N}_i}^t(k), \boldsymbol{\lambda}_{\mathcal{N}_i}(k), \boldsymbol{\mu}_{\mathcal{N}_i}(k)),$$

where functions $\boldsymbol{f}_i^x(\cdot), \boldsymbol{f}_i^\lambda(\cdot), \boldsymbol{f}_i^\mu(\cdot)$ denote the update functions of $\boldsymbol{x}_i^t, \boldsymbol{\lambda}_i, \boldsymbol{\mu}_i$, and $\boldsymbol{x}_{\mathcal{N}_i}^t(k), \boldsymbol{\lambda}_{\mathcal{N}_i}(k), \boldsymbol{\mu}_{\mathcal{N}_i}(k)$ signify the required information received from neighbors. Explicit expression of the update functions can be found in [22].

IV. Simulation and Experimental Results

In this section, we conduct extensive simulations and experiments to evaluate the robustness and scalability of the MAS-based hierarchical control framework. Given different time scales among the three control layers, we conduct simulations and experiments in decoupled control layers.

A. Robustness to Link Failures

In this subsection, we show that the MAS-based secondary control layer possesses higher robustness to link failures compared with the centralized secondary control layer. To demonstrate the concept, we implement a 4-agent DC Microgrid equipped with the droop-based primary control layer (3) and the consensus-like secondary control layer (5). The details of agent model can be found in [19]. The local reference voltages are chosen as $V_{ref1} = 48.2$V, $V_{ref2} = 48.3$V, $V_{ref3} = 47.9$V, and $V_{ref4} = 47.6$V. The local current loads are $I_{1L} = 10$A, $I_{2L} = 8$A, $I_{3L} = 12$A, and $I_{4L} = 6$A, and corresponding rated output currents are $I_1^* = 15$A, $I_2^* = 12$A, $I_3^* = 20$A, and $I_4^* = 12$A. Let V_i and $I_i, \forall i \in \mathcal{A} = \{1, 2, 3, 4\}$ be the output voltages and currents, respectively, then the two control objectives of the DC Microgrid can be formally introduced as

- Voltage balancing: $\frac{1}{4}\sum_{j\in\mathcal{A}} V_i = V_{ref}, V_{ref} = 48$V;
- Current sharing: $\frac{I_i}{I_i^*} = \frac{I_j}{I_j^*}, \forall i, j \in \mathcal{A}$.

Practically, link failures could be caused by random faults or dedicated attacks. Here we consider that the link will be out of service if it is in failure, i.e., the link is not able to transmit data packets. The MAS-based secondary control layer employs the consensus-like control algorithm, and the centralized secondary control layer relies a control center which can collect measurements from agents and send commands to them through communication links. We investigate the performance of the MAS-based and centralized secondary control layers under link failures:

1) The Centralized Secondary Control Layer: In this scenario, we consider that the communication link between agent 1 and control center is under failure. The result is shown in Fig. 3, where the AVGV is utilized to denote the average of $V_i, \forall i \in \mathcal{A}$.

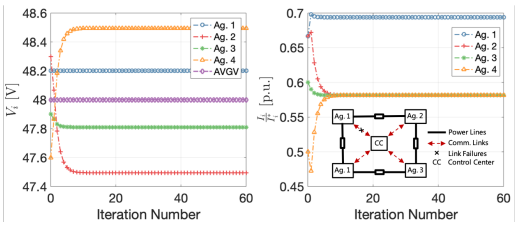

Fig. 3. This diagram shows output voltages and currents of the centralized secondary control layer, where the communication link connecting agent 1 and control center is under failure.

2) The MAS-based Secondary Control Layer: In this scenario, we consider that the communication link between agents 3 and 4 is under failure, as shown in Fig. 4.

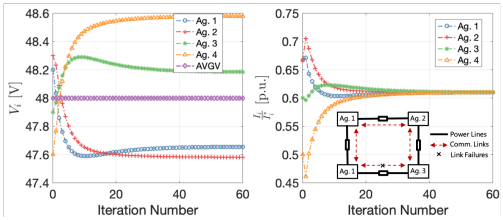

Fig. 4. This diagram shows output voltages and currents of the MAS-based secondary control layer, where the communication link between agents 3 and 4 is under failure.

According to Fig. 3, in the centralized secondary control layer, current sharing cannot be achieved in the DC Microgrid as the failed link isolates agent 1 from the remaining agents. However, as shown in Fig. 3, in the MAS-based secondary control layer, voltage balancing and current sharing can be eventually achieved even under the link failure, indicating that the MAS-based secondary control layer possesses higher robustness to link failures compared with the centralized secondary control layer. Moreover, the robustness to link failures can be quantified by communication graph's link-connectivity [23], which asks for the minimum number of links that need to be removed to make the remaining graph unconnected. The k-link-connectivity graph $\mathcal{G}$ can bear up to $k-1$ link failures.

B. Scalability

In this subsection, we choose to implement the MAS-based ACOPF collaborative solver in the tertiary control layer, and validate its correctness and scalability. We leverage the vast amount of processing cores and RAM provided by the HPC system at NC State University, called Henry2 cluster, to emulate the distributed computing environment required by the MAS-based collaborative ACOPF solver. Based on the HPC based distributed computing system, we test performances of the MAS-based solver in four test systems, i.e., 11 kV 22-bus [24], 12.7 kV 69-bus [25], 11 kV 85-bus [26], and 12.5kV 141-bus [27] radial distribution systems. The communication topology is considered to be identical as the physical system topology. The ACOPF solution references are obtained via three commonly used centralized optimization algorithms, i.e. interior point method (IPM), sequential quadratic programming (SQP) method, and active-set method (ASM).

First, we compare the ACOPF solution of the MAS-based algorithm with three benchmark algorithms, i.e. IPM, SQP, and ASM. The same convergence tolerance, i.e., 10^{-3} per unit, is used in the proposed MAS-based ACOPF algorithm and 3 benchmark algorithms. Once converged, we calculate the mean absolute error of the optimization variables $\boldsymbol{x}^t$ with respect to the three benchmark algorithms. The ACOPF solution accuracy comparisons between the reference algorithms and the MAS-based algorithm in every study system are summarized in TABLE I. We found that the mean absolute error of the MAS-based algorithm is on the 10^{-4} scale in average. According to the results in TABLE I, the MAS-based algorithm appears to be consistent with the reference algorithms, and we can conclude that the proposed MAS-based ACOPF algorithm is accurate.

TABLE I

MEAN ABSOLUTE ERRORS OF THE ACOPF SOLUTIONS.

	Versus IPM	Versus SQP	Versus ASM
22-bus	9.96×10^{-4}	9.47×10^{-4}	9.90×10^{-4}
69-bus	9.92×10^{-4}	9.39×10^{-4}	9.72×10^{-4}
85-bus	1.01×10^{-3}	1.12×10^{-3}	1.00×10^{-3}
141-bus	9.88×10^{-4}	8.99×10^{-4}	9.91×10^{-4}
Average	9.97×10^{-4}	9.76×10^{-4}	9.88×10^{-4}

To show the good scalability of the MAS-based collaborative ACOPF solver, we depict the computation time in the four test systems. As depicted in Fig. 5 (a), we can see that the total computation time, i.e. execution time, grows linearly as the system size grows. Additionally, the average agent receiving and sending data rate per iteration for all cases are plotted in Fig. 5 (b). We find that both data rates stay about the same. Since each agent only communicates with its 1-hop neighbor, the number of 1-hop neighbors does not grow as system size grows. The average 1-hop neighbors that each agent has in 4 cases are 1.91, 1.97, 1.98, and 1.99. The reason why this number is close to 2 is that majority of the agents only have one ancestor node and one children node, and some of the "endpoint" agent doesn't have children nodes. This contributes to the great scalability in Fig. 5 (b).

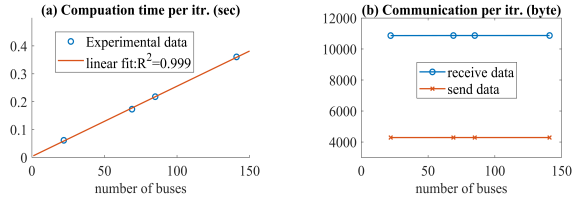

Fig. 5. Agent per iteration computation time and data rates.

V. CONCLUSION

In this paper, we proposed an MAS-based hierarchical control framework for Microgrids. Through extensive simulations and experiments, we showed that the proposed control framework demonstrated high robustness to link failures and good scalability. In future work, we plan to implement the MAS-based hierarchical control framework in the hardware-in-the-loop and real-world testbeds.

REFERENCES

[1] X. Liu and B. Su, "Microgrids—an integration of renewable energy technologies," in *2008 China International Conference on Electricity Distribution*. IEEE, 2008, pp. 1–7.

[2] A. G. Tsikalakis and N. D. Hatziargyriou, "Centralized control for optimizing microgrids operation," in *2011 IEEE power and energy society general meeting*. IEEE, 2011, pp. 1–8.

[3] N. Hatziargyriou, *Microgrids: architectures and control*. John Wiley & Sons, 2014.

[4] F. Katiraei, R. Iravani, N. Hatziargyriou, and A. Dimeas, "Microgrids management," *IEEE power and energy magazine*, vol. 6, no. 3, pp. 54–65, 2008.

[5] S. Hamilton, E. Gunther, R. Drummond, and S. E. Widergren, "Interoperability—a key element for the grid and der of the future," in *Proceedings of the IEEE Power Engineering Society Transmission and Distribution Conference*, 2006, pp. 927–931.

[6] J. M. Guerrero, J. C. Vasquez, J. Matas, L. G. De Vicuña, and M. Castilla, "Hierarchical control of droop-controlled ac and dc microgrids—a general approach toward standardization," *IEEE Transactions on industrial electronics*, vol. 58, no. 1, pp. 158–172, 2010.

[7] Y. F. Eddy, H. B. Gooi, and S. X. Chen, "Multi-agent system for distributed management of microgrids," *IEEE Transactions on power systems*, vol. 30, no. 1, pp. 24–34, 2014.

[8] Z. Cheng, J. Duan, and M.-Y. Chow, "To centralize or to distribute: That is the question: A comparison of advanced microgrid management systems," *IEEE Industrial Electronics Magazine*, vol. 12, no. 1, pp. 6–24, 2018.

[9] T. Logenthiran, D. Srinivasan, and A. M. Khambadkone, "Multi-agent system for energy resource scheduling of integrated microgrids in a distributed system," *Electric Power Systems Research*, vol. 81, no. 1, pp. 138–148, 2011.

[10] A. Bidram, A. Davoudi, F. L. Lewis, and Z. Qu, "Secondary control of microgrids based on distributed cooperative control of multi-agent systems," *IET Generation, Transmission & Distribution*, vol. 7, no. 8, pp. 822–831, 2013.

[11] J. Zhou, Y. Xu, H. Sun, L. Wang, and M. Y. Chow, "Distributed event-triggered h_∞ consensus based current sharing control of dc microgrids considering uncertainties," *IEEE Transactions on Industrial Informatics*, vol. 16, no. 12, pp. 7413–7425, 2020.

[12] J. Hu, A. Saleem, S. You, L. Nordström, M. Lind, and J. Østergaard, "A multi-agent system for distribution grid congestion management with electric vehicles," *Engineering Applications of Artificial Intelligence*, vol. 38, pp. 45–58, 2015.

[13] J. Duan and M. Chow, "A resilient consensus-based distributed energy management algorithm against data integrity attacks," *IEEE Transactions on Smart Grid*, vol. 10, no. 5, pp. 4729–4740, 2019.

[14] Z. Cheng and M. Y. Chow, "Resilient collaborative distributed energy management system framework for cyber-physical dc microgrids," *IEEE Transactions on Smart Grid*, vol. 11, no. 6, pp. 4637–4649, 2020.

[15] J. Duan and M. Chow, "Robust consensus-based distributed energy management for microgrids with packet losses tolerance," *IEEE Transactions on Smart Grid*, vol. 11, no. 1, pp. 281–290, 2020.

[16] S. D. McArthur, E. M. Davidson, V. M. Catterson, A. L. Dimeas, N. D. Hatziargyriou, F. Ponci, and T. Funabashi, "Multi-agent systems for power engineering applications—part i: Concepts, approaches, and technical challenges," *IEEE Transactions on Power systems*, vol. 22, no. 4, pp. 1743–1752, 2007.

[17] A. Bidram and A. Davoudi, "Hierarchical structure of microgrids control system," *IEEE Transactions on Smart Grid*, vol. 3, no. 4, pp. 1963–1976, 2012.

[18] K. Visscher and S. W. H. De Haan, "Virtual synchronous machines (vsg's) for frequency stabilisation in future grids with a significant share of decentralized generation," in *CIRED Seminar 2008: SmartGrids for Distribution*. IET, 2008, pp. 1–4.

[19] M. Tucci, L. Meng, J. M. Guerrero, and G. Ferrari-Trecate, "Stable current sharing and voltage balancing in dc microgrids: A consensus-based secondary control layer," *Automatica*, vol. 95, pp. 1–13, 2018.

[20] L. Gan, N. Li, U. Topcu, and S. H. Low, "Exact convex relaxation of optimal power flow in radial networks," *IEEE Transactions on Automatic Control*, vol. 60, no. 1, pp. 72–87, 2014.

[21] Y. Nesterov, "Primal-dual subgradient methods for convex problems," *Mathematical programming*, vol. 120, no. 1, pp. 221–259, 2009.

[22] Z. Cheng, "Resilient and secure collaborative distributed energy management system: a theoretical framework and applications in networked microgrids, [online] https://repository.lib.ncsu.edu/handle/1840.20/38358," Ph.D. dissertation, NC State University, 2020.

[23] H. J. LeBlanc, H. Zhang, X. Koutsoukos, and S. Sundaram, "Resilient asymptotic consensus in robust networks," *IEEE Journal on Selected Areas in Communications*, vol. 31, no. 4, pp. 766–781, 2013.

[24] M. Ramalinga Raju, K. Ramachandra Murthy, and K. Ravindra, "Direct search algorithm for capacitive compensation in radial distribution systems," *INT J ELEC POWER*, vol. 42, no. 1, pp. 24–30, Nov. 2012.

[25] D. Das, "Optimal placement of capacitors in radial distribution system using a Fuzzy-GA method," *INT J ELEC POWER*, vol. 30, no. 6-7, pp. 361–367, Jul. 2008.

[26] D. Das, D. Kothari, and A. Kalam, "Simple and efficient method for load flow solution of radial distribution networks," *INT J ELEC POWER*, vol. 17, no. 5, pp. 335–346, Oct. 1995.

[27] H. Khodr, F. Olsina, P. D. O.-D. Jesus, and J. Yusta, "Maximum savings approach for location and sizing of capacitors in distribution systems," *Electr. Power Syst. Res.*, vol. 78, no. 7, pp. 1192–1203, Jul. 2008.